

Field Driven Thermostated Systems : A Non-Linear Multi-Baker Map

T. Gilbert, C. D. Ferguson and J. R. Dorfman
*Department of Physics and Institute for Physical Science and Technology,
University of Maryland
College Park MD, 20742, USA
(November 14, 2018)*

In this paper, we discuss a simple deterministic model for a field driven, thermostated random walk that is constructed by a suitable generalization of a multi-baker map. The map is a usual multi-baker, but perturbed by a thermostated external field that has many of the properties of the fields used in systems with Gaussian thermostats. For small values of the driving field, the map is hyperbolic and has a unique SRB measure that we determine analytically to first order in the field parameter. We then compute the positive and negative Lyapunov exponents to second order and discuss their relation to the transport properties. For higher values of the parameter, this system becomes non-hyperbolic and possesses an attractive fixed point.

05.45 + b, 05.70 + Ln

I. INTRODUCTION

In the past several years a great deal of attention has been devoted to computer and analytic studies of the chaotic properties of fluid systems subjected to external fields and to Gaussian thermostats which maintain a constant kinetic or total energy in the system, in the presence of the field, [1,2]. The interest in this subject stems not only from the method's value as a means of simulating non-equilibrium flows and computing their properties, but also because there is a connection between transport properties, non-equilibrium fluctuations, and the underlying microscopically chaotic properties of the fluid. This connection has been explored from computational [3–8] and analytic [9–13] points of view. The purpose of this paper is to describe a model system in which the transport and dynamics of a thermostated system can be studied in great detail, and in which one can explicitly construct the SRB measure [14] and describe such properties as the transition from hyperbolic to non-hyperbolic behavior, and related phenomena. These properties have been explored in previous work [10,15], but have not yet been studied in great detail, due either to the complexity or to the simplicity of the models treated up till now [11–13]. The model discussed here allows one to gain some insights into the general class of properties of thermostated systems, while keeping the analytical and computational difficulties to manageable proportions. It is one of the few cases known so far where one can check

some of the general properties of thermostated systems on a specific model.

The model we consider is a variant of the multi-baker maps studied by Gaspard and coworkers [16–18], which are deterministic models for the diffusion of a particle on a one-dimensional lattice. The map considered here has, in addition, an external driving field which is constructed so as to model the effect of a thermostated electric field on charged particles in a two dimensional setting. We present the model and then calculate the chaotic properties at small values of the external field. We obtain an expression for the stationary state SRB measure to first order in the applied field, and the positive and negative Lyapunov exponents to second order in the applied field. This allows us to verify the interesting relations between the rate of entropy production, the zero field diffusion coefficient, the drift velocity, and the sum of the Lyapunov exponents [2,10,12,13]. We conclude with a brief discussion of the transition to non-hyperbolic behavior as the field increases beyond a certain value, and discuss the connection of our model to other types of field-driven multi-baker maps [11–13].

II. THE NON-LINEAR MULTI-BAKER MAP

We begin by considering a simple multibaker map that acts on the (x, y) -coordinates of particles, and that models a random walk on a one-dimensional lattice of unit spacing. The map, defined on $\mathbf{Z} \times [0, 1]^2$, replaces the n, x, y coordinates of a particle by $M_0(n, x, y)$

$$\begin{aligned} M_0(n, x, y) &= (n - 1, 2x, \frac{y}{2}), & 0 \leq x < 1/2, \\ &= (n + 1, 2x - 1, \frac{y + 1}{2}), & 1/2 \leq x < 1. \end{aligned} \quad (1)$$

Here n represents the position of the random walker on the line and x, y can be seen as bookkeeping variables keeping track of the deterministic cause of the apparent random walk. The subscript, zero, on M indicates that this is the map defined without an external field, which we introduce shortly. The map M_0 is time reversal symmetric. That is, there exists an involution operator, T , which acts on the x, y -variables, but not on the box index n , and is given by $T(x, y) = (1 - y, 1 - x)$, with $T^2 = \mathbf{1}$, where $\mathbf{1}$ is the identity operator in \mathbf{R}^2 , and such that $T \circ M_0 \circ T(n, x, y) = M_0^{-1}(n, x, y)$. If we consider

periodic boundary conditions, the invariant measure is uniform and has Lyapunov exponents

$$\lambda_+^{(0)} = -\lambda_-^{(0)} = \ln 2. \quad (2)$$

Next we suppose that the particles are also acted upon by a thermostated electric field, whose action we now model. Our final map will then be a composition (to be explained below) of the field map (3) with the multi-baker map (1).

The modelling of the field map can be done by considering the action of a thermostated electric field on a (continuously) moving particle, where the thermostat maintains a constant kinetic energy for the particle. The equation of motion of a particle in such a field is given by [1,2]

$$\frac{d\vec{p}}{dt} = q\vec{E} - q \left(\frac{\vec{E} \cdot \vec{p}}{p^2} \right) \vec{p}.$$

If θ is the angle that the particle makes with respect to the direction of the electric field, then θ changes in time as $\dot{\theta} = -qE \sin \theta / p$, with solution

$$\theta(t) = 2 \arctan \left(\tan \left(\frac{\theta(0)}{2} \right) \exp \left(-\frac{qE}{p} t \right) \right).$$

A time discretized version of this equation is obtained by defining an angle at discrete times $\theta_n = \pi x_n$, and letting x_n satisfy

$$x_{n+1} = \frac{2}{\pi} \arctan \left(\tan \left(\frac{\pi x_n}{2} \right) e^{-\alpha} \right).$$

Here $x_n \in [0, 1]$ and $\alpha = \frac{qE}{p} \tau$, with τ the time step, which for the time being we set equal to unity. Note that we restricted our attention to angles $\theta \in [0, \pi]$, taking advantage of the symmetry $\theta \leftrightarrow -\theta$.

We now introduce a one parameter family of maps of the unit interval onto itself by

$$\varphi_\alpha(x) = \frac{2}{\pi} \arctan \left(\tan \left(\frac{\pi x}{2} \right) e^{-\alpha} \right). \quad (3)$$

We note the following property :

$$\varphi_\alpha(x) = 1 - \varphi_{-\alpha}(1 - x), \quad (4)$$

which implies the time reversal symmetry

$$T \circ (\varphi_\alpha, \mathbf{1}) \circ T(x, y) = (x, \varphi_\alpha^{-1}(y)), \quad (5)$$

where T is defined above, and the operator $(\varphi_\alpha, \mathbf{1})$ acts on a point (x, y) , say to produce $(\varphi_\alpha(x), y)$, and we have denoted the identity operator acting on the y -coordinate by $\mathbf{1}$. We also point out the fact that the map $\varphi_\alpha(x)$ has the property, under successive iterations, that

$$\varphi_\alpha(\varphi_\alpha(x)) = \varphi_{2\alpha}(x), \quad (6)$$

which shows that the field map is a good discretization of a continuous process in time.

We can now construct the following non-linear (or field driven) multi-baker map as a time reversal symmetric composition of the multi-baker map (1) with the field map (3) :

$$M_\alpha(n, x, y) = (\mathbf{1}, \mathbf{1}, \varphi_\alpha) \circ M_0 \circ (\mathbf{1}, \varphi_\alpha, \mathbf{1})(n, x, y), \quad (7)$$

which takes the explicit form

$$\begin{aligned} M_\alpha(n, x, y) &= (n - 1, 2\varphi_\alpha(x), \varphi_\alpha(\frac{y}{2})), \\ &0 \leq x < \varphi_{-\alpha}(\frac{1}{2}), \\ &= (n + 1, 2\varphi_\alpha(x) - 1, \varphi_\alpha(\frac{y+1}{2})), \\ &\varphi_{-\alpha}(\frac{1}{2}) \leq x < 1. \end{aligned} \quad (8)$$

The leftmost identity operators in each of the field maps in (7) act on the cell index, n , and express the fact that the field maps do not change the value of the cell index. Only the baker map moves points from one cell to the next. We refer to Fig. (5) at the end of this paper for an illustration of the projection of M_α along the x -interval. The time reversal symmetry of this map $T \circ M_\alpha \circ T(x, y) = M_\alpha^{-1}(x, y)$, with T defined as above, follows straightforwardly from (4, 5).

III. HYPERBOLIC REGIME

As long as $\alpha < \ln(2)$, M_α is expanding along the x -direction, i.e.

$$\frac{\partial M_{\alpha x}}{\partial x} > 1,$$

so that standard theorems guarantee the existence and uniqueness of an SRB measure [19]. In this section we solve for the invariant density and give an analytic expression of this invariant measure.

We want to find the stationary eigenfunction, equivalently, the invariant density, $\rho(n, x, y)$, of the Perron-Frobenius operator for a system with periodic boundary conditions. This implies that ρ does not depend upon n , but only on x, y and satisfies the equation

$$\begin{aligned} \rho(x, y) &= \varphi'_{-\alpha}(\frac{x}{2}) \varphi'_{-\alpha}(y) \rho(\varphi_{-\alpha}(\frac{x}{2}), 2\varphi_{-\alpha}(y)), \\ &0 \leq y < \varphi_\alpha(\frac{1}{2}), \\ &= \varphi'_{-\alpha}(\frac{x+1}{2}) \varphi'_{-\alpha}(y) \rho(\varphi_{-\alpha}(\frac{x+1}{2}), 2\varphi_{-\alpha}(y) - 1), \\ &\varphi_\alpha(\frac{1}{2}) \leq y < 1 \end{aligned} \quad (9)$$

where the prime denotes the derivation with respect to the argument. We solve this equation by expanding the density in powers of the field parameter,

$$\rho(x, y) \simeq 1 + \alpha \rho^{(1)}(x, y) + \alpha^2 \rho^{(2)}(x, y) + o(\alpha^3). \quad (10)$$

For small α , the low field regime, we expand φ_α in powers of the field parameter :

$$\varphi_\alpha(x) \simeq x - \frac{\alpha}{\pi} \sin(\pi x) + \frac{\alpha^2}{4\pi} \sin(2\pi x) + o(\alpha^3). \quad (11)$$

The first order correction to the invariant density is found by decomposing it in Fourier modes :

$$\rho^{(1)}(x, y) = \sum_{k=0}^{\infty} [a_k(y) \cos(2\pi kx) + b_k(y) \sin(2\pi kx)]. \quad (12)$$

Inserting the expansion for ρ , Eq. (10), and Eq. (12) in Eq. (9), we can find the a_k 's and b_k 's. However, as a result of the phase space contraction, the density is a singular function of the y coordinate so that we cannot represent the a_k 's and b_k 's in terms of standard functions [20]. For our purposes, it is enough to perform a partial integration of the density along the y direction so as to obtain continuous coefficients for the Fourier modes. We thus define

$$A_k(y) = \int_0^y a_k(y') dy'; \quad B_k(y) = \int_0^y b_k(y') dy'. \quad (13)$$

which, to lowest order in α , are found to satisfy the recursion relations

$$\begin{aligned} A_0(y) &= \frac{1}{2} A_0(2y) + \frac{2y}{\pi} + \frac{1}{\pi} \sin(\pi y) \\ &\quad + \frac{1}{\pi} \sum_{k' \text{ odd}} \frac{B_{k'}(2y)}{k'}, \\ &\hspace{15em} 0 \leq y < \frac{1}{2}, \\ &= \frac{1}{2} A_0(2y-1) + \frac{2(1-y)}{\pi} + \frac{1}{\pi} \sin(\pi y) \\ &\quad + \frac{1}{\pi} \sum_{k' \text{ odd}} \left(\frac{B_{k'}(1)}{k'} - \frac{B_{k'}(2y-1)}{k'} \right), \\ &\hspace{15em} \frac{1}{2} \leq y < 1, \end{aligned} \quad (14)$$

$$\begin{aligned} A_k(y) &= \frac{1}{2} A_{2k}(2y) - \frac{y}{\pi(4k^2-1/4)} \\ &\quad - \frac{2}{\pi} \sum_{k' \text{ odd}} \frac{k'}{4k^2-k'^2} B_{k'}(2y), \\ &\hspace{15em} 0 \leq y < \frac{1}{2} \\ &= \frac{1}{2} (A_{2k}(1) + A_{2k}(2y-1)) - \frac{1-y}{\pi(4k^2-1/4)} \\ &\quad - \frac{2}{\pi} \sum_{k' \text{ odd}} \frac{k'}{4k^2-k'^2} (B_{k'}(1) - B_{k'}(2y-1)), \\ &\hspace{15em} \frac{1}{2} \leq y < 1, \end{aligned} \quad (15)$$

$$\begin{aligned} B_k(y) &= \frac{1}{2} B_{2k}(2y) + \frac{4ky}{\pi(4k^2-1/4)} \\ &\quad + \frac{4k}{\pi} \sum_{k' \text{ odd}} \frac{1}{4k^2-k'^2} A_{k'}(2y), \\ &\hspace{15em} 0 \leq y < \frac{1}{2}, \\ &= \frac{1}{2} (B_{2k}(1) + B_{2k}(2y-1)) + \frac{4ky}{\pi(4k^2-1/4)} \\ &\quad + \frac{4k}{\pi} \sum_{k' \text{ odd}} \frac{1}{4k^2-k'^2} (A_{k'}(1) - A_{k'}(2y-1)), \\ &\hspace{15em} \frac{1}{2} \leq y < 1. \end{aligned} \quad (16)$$

In particular, for $y = 1$, we find $A_k(1) = A_{2k}(1)$ and $B_k(1) = B_{2k}(1) + \frac{4k}{\pi(4k^2-1/4)}$, whose solutions are, respectively,

$$A_k(1) = 0; \quad B_k(1) = \frac{4}{\pi} \sum_{n=0}^{\infty} \frac{2^n k}{2^{2(n+1)} k^2 - 1/4} \quad (17)$$

Therefore the projection of $\rho^{(1)}(x, y)$ along the x -direction, is a smooth function of x given by

$$\rho^{(1)}(x) \equiv \int_0^1 \rho^{(1)}(x, y) dy = \sum_{k=1}^{\infty} B_k(1) \sin(2\pi kx). \quad (18)$$

To compute the coefficients $A_k(y)$ and $B_k(y)$ numerically, we need to select a cut-off value k_{max} of k beyond which we set all the coefficients to be zero. In Figs. (1)-(3), we show A_0 and the first five A_k 's and B_k 's, respectively, computed by setting $k_{max} = 250$.

Although we have found the invariant density only to first order, we can now compute the corrections to the Lyapunov exponents to second order in α . For λ_+ , we obtain

$$\begin{aligned} \lambda_+ &= \int_0^1 dx \int_0^1 dy \rho(x, y) \ln(2\varphi'_\alpha(x)) \\ &= \ln(2) - \alpha^2 \left(\frac{1}{4} + \int_0^1 dx \rho^{(1)}(x) \cos(\pi x) \right) \\ &= \ln(2) - \alpha^2 \left(\frac{1}{4} + \frac{4}{\pi} \sum_{k=1}^{\infty} \frac{k B_k(1)}{4k^2-1} \right) \\ &= \lambda_+^{(0)} - \alpha^2 (0.6661513 \pm 10^{-7}). \end{aligned} \quad (19)$$

Here we used the normalization condition for $\rho(x, y)$ which requires that

$$\int_0^1 dx \int_0^1 dy \rho^{(2)}(x, y) = 0. \quad (20)$$

To compute λ_- , we need the full expression of $\rho^{(1)}$, Eqs. (12-16) :

$$\begin{aligned}
\lambda_- &= \int_0^{\varphi_{-\alpha}(1/2)} dx \int_0^1 dy \rho(x, y) \ln\left(\frac{1}{2}\varphi'_\alpha(y/2)\right) \\
&\quad + \int_{\varphi_{-\alpha}(1/2)}^1 dx \int_0^1 dy \rho(x, y) \ln\left(\frac{1}{2}\varphi'_\alpha((y+1)/2)\right) \\
&= \varphi_{-\alpha}(1/2) \left(-\ln(2) - \frac{2\alpha}{\pi} - \frac{\alpha^2}{4}\right) \\
&\quad - \alpha^2 \int_0^{1/2} dx \int_0^1 dy \rho_1(x, y) \cos(\pi y/2) \\
&\quad + (1 - \varphi_{-\alpha}(1/2)) \left(-\ln(2) + \frac{2\alpha}{\pi} - \frac{\alpha^2}{4}\right) \\
&\quad + \alpha^2 \int_{1/2}^1 dx \int_0^1 dy \rho_1(x, y) \sin(\pi y/2) \\
&= \lambda_-^{(0)} - \alpha^2 \left(\frac{1}{4} + \frac{4}{\pi^2} + \frac{1}{\pi} \sum_{k \text{ odd}} \frac{B_k(1)}{k}\right. \\
&\quad + \frac{\pi}{4} \int_0^1 dy A_0(y) (\sin(\pi y/2) + \cos(\pi y/2)) \\
&\quad \left. + \frac{1}{2} \int_0^1 dy \sum_{k \text{ odd}} \frac{B_k(y)}{k} (\sin(\pi y/2) - \cos(\pi y/2))\right). \tag{21}
\end{aligned}$$

It is not straightforward to compute these integrals numerically because of the irregularity of the functions (14-16) and the number of different terms involved in their expressions. We can nevertheless estimate (21) within some good accuracy. To this purpose, we proceed by a number of algebraic manipulations.

We first substitute for $B_k(y)$ the expression

$$B_k(y) = yB_k(1) + kf_k(y), \tag{22}$$

where the functions $f_k(y)$ are found to satisfy the relations

$$f_k(y) = f_{2k}(2y) + \frac{4}{\pi} \sum_{k' \text{ odd}} \frac{1}{4k^2 - k'^2} A_{k'}(2y), \tag{23}$$

for $0 \leq y < 1/2$, and $f_k(y)$ is odd with respect to $1/2$, viz. $f_k(y) = -f_k(1-y)$.

In terms of these, we have

$$\begin{aligned}
A_k(y) &= \frac{1}{2} A_{2k}(2y) - \frac{2}{\pi} \sum_{k' \text{ odd}} \frac{k'^2}{4k^2 - k'^2} f_{k'}(2y) \\
&\quad - \frac{y}{\pi} \left(\frac{4}{16k^2 - 1} + \sum_{k' \text{ odd}} \frac{4k'}{4k^2 - k'^2} B_{k'}(1)\right), \tag{24}
\end{aligned}$$

for $0 \leq y < 1/2$, and $A_k(y)$ is even with respect to $1/2$, viz. $A_k(y) = A_k(1-y)$.

We can now find an upper bound on the magnitude of $f_k(y)$. Indeed, $A_k(y)$ is everywhere negative and is minimal at $y = 1/2$ (see Fig.(2)). Thus

$$|A_k| \leq \frac{1}{2\pi} \left(\frac{4}{16k^2 - 1} + \sum_{k' \text{ odd}} \frac{4k'}{4k^2 - k'^2} B_{k'}(1)\right). \tag{25}$$

Now, $f_k(y)$ is negative between 0 and $1/2$ and reaches its minimum at $y = 1/4$. Thus, from Eqs. (23, 25),

$$\begin{aligned}
|f_k| &\leq f_k^{max} \equiv \frac{2}{\pi^2} \sum_{k' \text{ odd}} \frac{1}{4k^2 - k'^2} \\
&\quad \times \left(\frac{4}{16k^2 - 1} + \sum_{k' \text{ odd}} \frac{4k'}{4k^2 - k'^2} B_{k'}(1)\right). \tag{26}
\end{aligned}$$

Next, we rewrite $A_0(y)$, Eq. (14), in terms of its Fourier modes :

$$A_0(y) = \frac{1}{\pi} \sum_{k=0}^{\infty} G_k \cos(2\pi ky) + H_k \sin(2\pi ky). \tag{27}$$

We find

$$\begin{aligned}
G_0 &= 1 + \frac{4}{\pi} + \sum_{k' \text{ odd}} \frac{B_{k'}(1)}{k'} \\
G_k &= -\frac{4}{\pi^2 k^2} \left(1 + \sum_{k' \text{ odd}} \frac{B_{k'}(1)}{k'}\right) - \frac{4}{\pi(4k^2 - 1)} \\
&\quad + 2 \sum_{k' \text{ odd}} \int_0^1 dy f_{k'}(y) \cos(k\pi y), \quad k \text{ odd}, \\
G_k &= \frac{1}{2} G_{k/2} - \frac{4}{\pi(4k^2 - 1)}, \quad k \text{ even}, \\
H_k &= 0, \quad k \text{ odd}, \\
H_k &= -\frac{4}{\pi k} \sum_{k' \text{ odd}} \frac{B_{k'}(1)}{k'} + 2 \sum_{k' \text{ odd}} \int_0^1 dy f_{k'}(y) \sin(k\pi y), \\
&\quad k \text{ even}, \tag{28}
\end{aligned}$$

Therefore and with the help of Eqs.(25, 26),

$$\begin{aligned}
&\int_0^1 dy \sum_{k \text{ odd}} \frac{B_k(y)}{k} (\sin(\pi y/2) - \cos(\pi y/2)) \\
&= \frac{2}{\pi} \left(\frac{4}{\pi} - 1\right) \sum_{k \text{ odd}} \frac{B_k(1)}{k} \\
&\quad + \sum_{k \text{ odd}} \int_0^1 dy f_k(y) (\sin(\pi y/2) - \cos(\pi y/2)) \\
&= \frac{2}{\pi} \left(\frac{4}{\pi} - 1\right) \sum_{k \text{ odd}} \frac{B_k(1)}{k} + O\left(\frac{4}{\pi}(\sqrt{2} - 1)f_k^{max}\right), \tag{29}
\end{aligned}$$

and

$$\begin{aligned}
&\int_0^1 dy A_0(y) (\sin(\pi y/2) + \cos(\pi y/2)) \\
&= \frac{4G_0}{\pi^2} - \frac{4}{\pi^2} \sum_{k=1}^{\infty} \frac{G_k}{16k^2 - 1} \\
&= \frac{4G_0}{\pi^2} - \frac{4}{\pi^2} \sum_{k \text{ odd}} \left(\sum_{n=0}^{\infty} \frac{1}{2^n} \frac{G_k}{2^{2n+4}k^2 - 1}\right)
\end{aligned}$$

$$\begin{aligned}
& + \sum_{n=1}^{\infty} \sum_{j=0}^{n-1} \frac{1}{2^j} \frac{g_{2^{n-j}k}}{2^{2n+4}k^2 - 1} \Big) \\
= & \frac{4G_0}{\pi^2} - \frac{4}{\pi^2} \sum_{k \text{ odd}} \left(\sum_{n=0}^{\infty} \frac{1}{2^n} \frac{G_k^{(0)}}{2^{2n+4}k^2 - 1} \right. \\
& \left. + \sum_{n=1}^{\infty} \sum_{j=0}^{n-1} \frac{1}{2^j} \frac{g_{2^{n-j}k}}{2^{2n+4}k^2 - 1} \right) \\
& + O \left(\frac{4}{\pi^2} \sum_{k \text{ odd}} \sum_{n=0}^{\infty} \frac{1}{2^{n-1}} \frac{1}{2^{2n+4}k^2 - 1} \right. \\
& \quad \left. \times \frac{2}{\pi} \sum_{k' \text{ odd}} \frac{f_{k'}^{max}}{k'} \right), \quad (30)
\end{aligned}$$

where we introduced the notations

$$G_k^{(0)} = -\frac{4}{\pi^2 k^2} \left(1 + \sum_{k' \text{ odd}} \frac{B_{k'}(1)}{k'} \right) - \frac{4}{\pi(4k^2 - 1)} \quad (31)$$

and

$$g_{2^{n-j}k} = -\frac{4}{\pi(2^{2(n-j+1)}k^2 - 1)}. \quad (32)$$

Grouping Eqs.(29, 30) together with Eq.(21), we can give an estimate of the second order correction to the negative Lyapunov exponent by performing straightforward numerical summations : we find

$$\lambda_- = \lambda_-^{(0)} - \alpha^2(1.9937 \pm O(0.04)). \quad (33)$$

In Fig. (4) we compare the values (19) and (33) of the second order corrections to the Lyapunov exponents to numerically computed ones.

In the next section we take the macroscopic limit and relate the sum of the Lyapunov exponents to the drift velocity and the zero-field diffusion coefficient.

IV. MACROSCOPIC LIMIT

In order to take the macroscopic limit of this diffusive process, we consider the function $W_t(n)$ which is defined to be the total probability of finding a particle in cell n at time t , and is given by

$$W_t(n) = \int_0^1 dx \int_0^1 dy \rho_t(n, x, y), \quad (34)$$

where $\rho_t(n, x, y)$ is the time-dependent density of the extended version of M_α and whose time evolution is derived by generalizing Eq. (9) in a straightforward way. Once we have eliminated the internal variables, (x, y) , we no longer have a deterministic process, but instead have a random process which should, in a macroscopic limit, be described by a suitable Fokker-Planck equation with a

drift term, representing the effect of the external field. The macroscopic limit is taken by scaling the space and time parameters, and then taking an appropriate scaling limit. This procedure was described for models of this type by Tél, Vollmer, and Breyman [11,12], and here we simply outline the process.

We have previously introduced the time step τ , and we replace the times t and $t + 1$ in the Frobenius-Perron equation by $T\tau$ and $T\tau + \tau$, respectively, where $T \gg 1$. Similarly, we scale the length of the elementary cells, n , by making them have a length a on a side. We then replace n and $n + 1$ in the Frobenius-Perron equation by Na and $Na + a$, respectively, where $N \gg 1$. Also the x and y variables have to be scaled by the factor a , as well.

We can now proceed to the derivation of the Fokker-Planck equation from the Frobenius-Perron equation for $\rho_t(n, x, y)$. We obtain a Fokker-Planck equation for a field-driven random walk by considering the difference $W_{T\tau+\tau}(Na) - W_{T\tau}(Na)$.

Using Eqs. (8,9), we find

$$\begin{aligned}
W_{T\tau+\tau}(Na) = & \int_0^{\varphi-\alpha(1/2)} dx \rho_{T\tau}(Na + a, x) \\
& + \int_{\varphi-\alpha(1/2)}^1 dx \rho_{T\tau}(Na - a, x),
\end{aligned}$$

where $\rho_{T\tau}(Na, x) = a \int_0^1 dy \rho_{T\tau}(Na, x, y)$. We have scaled x and y so that their values are in the interval $0 \leq x, y \leq 1$. Therefore,

$$\begin{aligned}
W_{T\tau+\tau}(Na) - W_{T\tau}(Na) = & \int_0^{\varphi-\alpha(1/2)} dx (\rho_{T\tau}(Na + a, x) - \rho_{T\tau}(Na, x)) \\
& + \int_{\varphi-\alpha(1/2)}^1 dx (\rho_{T\tau}(Na - a, x) - \rho_{T\tau}(Na, x)). \quad (35)
\end{aligned}$$

Expanding $\rho_{T\tau}(Na \pm a, x)$ about $\rho_{T\tau}(Na, x)$ and $W_{T\tau+\tau}(Na)$ about $W_{T\tau}(Na)$ respectively, and introducing the coordinate $X = Na$, and the time $t = T\tau$, we get

$$\begin{aligned}
\frac{\partial W_t(X)}{\partial t} = & \frac{a}{\tau} \frac{\partial}{\partial X} \left(\int_0^{\varphi-\alpha(1/2)} dx \rho_t(X, x) - \int_{\varphi-\alpha(1/2)}^1 dx \rho_t(X, x) \right) + a^2 \frac{1}{2\tau} \frac{\partial^2 W_t(X)}{\partial X^2} + \dots \\
= & -\bar{v}_t(X) \frac{\partial W_t(X)}{\partial X} + \frac{a^2}{2\tau} \frac{\partial^2 W_t(X)}{\partial X^2} + \dots \quad (36)
\end{aligned}$$

The *drift velocity* is given by,

$$\bar{v}_t(X) \equiv \frac{a}{\tau} \times$$

$$\frac{\frac{\partial}{\partial X} \left(- \int_0^{\varphi_{-\alpha}(1/2)} dx \rho_t(X, x) + \int_{\varphi_{-\alpha}(1/2)}^1 dx \rho_t(X, x) \right)}{\frac{\partial}{\partial X} \int_0^1 dx \rho_t(X, x)} \quad (37)$$

To proceed further, we need to take the macroscopic limit where $a \rightarrow 0, \tau \rightarrow 0, \frac{a^2}{2\tau} = D$ and \bar{v} is finite and nonzero. This implies that the electric field, E , becomes infinite as a^{-2} .

For long times, t , we are going to replace the drift velocity in the Fokker-Planck equation by its stationary state value. Suppose t is large enough that we are nearing a steady state. Then in the limit of small a and τ , we may write the solution of the Frobenius-Perron equation $\rho_t(X, x)$ in (37) as $W_t(X)\rho(x)$ where $\rho(x)$ is determined by an equation easily obtained by integrating the equation (9) over y (18), and $W_t(X)$ is close to, but not quite, a constant. Then the X dependence drops out in the expression for the drift velocity, and we find that the stationary state drift velocity is simply (assuming that the density is normalized to a unit cell)

$$\bar{v} = \frac{a}{\tau} \left(- \int_0^{\varphi_{-\alpha}(1/2)} dx \rho(x) + \int_{\varphi_{-\alpha}(1/2)}^1 dx \rho(x) \right). \quad (38)$$

Eq. (36) is the Fokker-Planck equation corresponding to a stochastic diffusive system with a drift. In the case of *periodic* boundary conditions that we consider here, we know from thermodynamics that the rate of entropy production in the stationary state is due solely to the existence of a current driven by the external field and for which the rate of entropy production is given by

$$\sigma = \frac{\bar{v}^2}{D}, \quad (39)$$

where the zero-field diffusion coefficient for this process is $D = \frac{a^2}{2\tau}$. We mention that in the limit of zero field, and periodic boundary conditions, the entropy production in the stationary state vanishes, since in this limit, there is no steady state drift, and the distribution function $\rho(X, x)$ is constant both in X and in x .

With the stationary state density (18) computed in the previous section, the drift velocity (38) is found to be

$$\begin{aligned} \bar{v} &= -\frac{2a\alpha}{\pi\tau} \left(1 + \sum_{k \text{ odd}} \frac{B_k(1)}{k} \right) \\ &= -\frac{a\alpha}{\tau} (1.15217813). \end{aligned} \quad (40)$$

Hence, the entropy production rate is, Eqs. (39 - 40),

$$\sigma = 2.65502889 \frac{\alpha^2}{\tau}. \quad (41)$$

According to the usual arguments for thermostated systems, one expects that the rate of phase space contraction

given by the negative of the sum of Lyapunov exponents should be equal to the macroscopic rate of entropy production [10,13]. For our case, it is possible to verify this relation analytically, since we have been able to calculate all of the relevant quantities. The phase space contraction rate is given by

$$-(\lambda_+ + \lambda_-) = (2.66 \pm O(0.04)) \frac{\alpha^2}{\tau}, \quad (42)$$

and Eqs. (41,42) give constant values. Thus, our field driven random walk model has a well behaved macroscopic limit, provides an example of the correspondence between the macroscopic and microscopic relations for entropy production, and is analytically tractable.

V. CONCLUSIONS AND DISCUSSION

In this paper, we have shown that it is possible to construct a non-linear version of the multibaker map (i.e. it shares the topology and time-reversal symmetry of the original multi-baker but is not piecewise linear) that simulates the action of an external field on a diffusive process. The field curves the branches of the map and is responsible for the phase space contraction that induces a stationary state on an attractor (it fills the whole phase space but its information dimension [14] is fractional as a consequence of the difference between the second order corrections to the Lyapunov exponents).

One of the motivations of this work was to provide an analytically tractable map which shows some of the properties of the periodic Lorentz gas where the particle moves among the scatterers in a thermostated electric field. The structure of our non-linear baker map is sufficiently simple that we were able to compute analytically the stationary state SRB measure using a perturbation expansion in the field parameter. This allowed us to compute the positive and negative Lyapunov exponents, whose values we showed are consistent with that of the drift velocity. We also were able to compute the irreversible entropy production and showed that it is indeed given, apart from some factors, by the sum of the Lyapunov exponents.

We remark that at values of the field parameter larger than $\ln(2)$, the map loses its hyperbolicity. This is illustrated in Fig. (5). In fact (0,0) becomes an attractive fixed point of the reduced map, which means that, on the lattice, all particles eventually move ballistically around the ring towards decreasing n 's. The case $\alpha = \ln(2)$ is of particular interest. Indeed, the origin is an intermittent fixed point and, as a consequence, points can spend arbitrary long times in its vicinity. This can be seen to give rise to anomalous diffusion [21,22].

We regard the model given here as the simplest of a class of similar models which can be generated by varying an additional parameter modelling a magnetic field. Elsewhere [23] we will describe this class of models in

much more detail, because they show a wide variety of features both in the hyperbolic and non-hyperbolic regions, including sequences of period adding bifurcations.

In a subsequent paper [24] we will consider boundary conditions other than periodic. It is in particular an important question to check whether, with flux boundary conditions, the chain sustains a stationary state with an almost linear gradient of density. As we showed in another paper [13], some other models of field driven multi-baker maps fail to have this behavior in a large system limit and, as a consequence, do not have physically relevant thermodynamics (the entropy production rate depends on the choice of the partition).

Another interesting perspective will be to calculate non linear corrections to the diffusion coefficient so we can go beyond the linear response theory. As shown by other authors [18], relevant tools for this study are the zeta functions and Pollicott-Ruelle resonances. Computing the first order corrections to the eigenvalue spectrum of the Perron-Frobenius operator will be an important step towards understanding non-linear diffusion for this model.

ACKNOWLEDGMENTS

The authors wish to thank Brian Hunt, Celso Grebogi, Jurgen Vollmer, Tamas Tél, Rainer Klages, Edward Ott, Karol Życzkowski and Mihir Arjunwadkar for helpful discussions, and Pierre Gaspard, Shuichi Tasaki, and Constantino Tsallis for pointing out the interesting intermittent behavior at the hyperbolic-nonhyperbolic transition. J. R. D. wishes to acknowledge support from the National Science Foundation under grant PHY -96 -00428.

[1] W. G. Hoover, *Computational Statistical Mechanics* (Elsevier Science Publishers, Amsterdam, 1991).
 [2] D. J. Evans and G. P. Morriss, *Statistical Mechanics of Non-Equilibrium Fluids* (Academic Press, London, 1990).
 [3] H. A. Posch and W. G. Hoover, *Lyapunov Instability of Dense Lennard-Jones Fluids*, Phys. Rev. A **38**, 473 (1988).
 [4] D. J. Evans, E. G. D. Cohen and G. P. Morriss, Phys. Rev. A **42**, 5990 (1990).
 [5] D. J. Evans, E. G. D. Cohen and G. P. Morriss, Phys. Rev. Lett. **71**, 2401 (1993).
 [6] A. Baranyai, D. J. Evans and E. G. D. Cohen, J. Stat. Phys. **70**, 1085 (1993).
 [7] G. P. Morriss, C. P. Dettmann, and L. Rondoni, *Recent Results for the Thermostatted Lorentz Gas*, Physica A **240**, 84, (1997).
 [8] G. P. Morriss and C. P. Dettmann, *Thermostats: Analysis and Application*, Chaos, **8**, 321, (1998).
 [9] N. I. Chernov, G. L. Eyink, J. L. Lebowitz and Ya. G.

Sinai, *Steady State Electric Conductivity in the Periodic Lorentz Gas*, Com. Math. Phys. **154**, 569 (1993).
 [10] D. Ruelle, *Positivity of Entropy Production in Nonequilibrium Statistical Mechanics*, J. Stat. Phys. **85**, 1 (1996).
 [11] W. Breyermann, T. Tél and J. Vollmer, *Entropy Production for Open Dynamical Systems*, Phys. Rev. Lett. **77**, 2945 (1996).
 [12] T. Tél, J. Vollmer and W. Breyermann, *Transient Chaos : the Origin of Transport in Driven Systems*, Europhys. Lett. **35**, 659 (1996); J. Vollmer, T. Tél and W. Breyermann, *Equivalence of Irreversible Entropy Production in Driven Systems : an Elementary Chaotic Map Approach*, Phys. Rev. Lett. **79**, 2759 (1997). W. Breyermann, T. Tél, and J. Vollmer, *Entropy Balance, Time Reversibility, and Mass Transport in Dynamical Systems*, Chaos **8**, 396, (1998). J. Vollmer, T. Tél and W. Breyermann, *Entropy balance in the presence of drift and diffusion currents : an elementary chaotic map approach*, Phys. Rev. E **58**, 1672 (1998).
 [13] T. Gilbert and J. R. Dorfman, *Entropy Production : From Open Volume Preserving to Dissipative Systems*, submitted to J. Stat. Phys. (1998), archived at *chaodyn/9804009*.
 [14] J.-P. Eckmann and D. Ruelle, *Ergodic Theory of Chaos and Strange Attractors*, Rev. Mod. Phys. **57**, 617 (1985).
 [15] D. Ruelle, *New Theoretical Ideas in Nonequilibrium Statistical Mechanics*, Lecture notes Rutgers U. and I. H. E. S. (1997), unpublished.
 [16] S. Tasaki and P. Gaspard, *Fick's Law and Fractality of Nonequilibrium Stationary States in a Reversible Multi-baker Map*, J. Stat. Phys. **81**, 935 (1995).
 [17] P. Gaspard, *Entropy Production in Open, Volume Preserving Systems*, J. Stat. Phys. **89**, 1215 (1997).
 [18] P. Gaspard, *Chaos, Scattering, and Statistical Mechanics* (Cambridge University Press, Cambridge, 1998).
 [19] A. Boyarsky and P. Góra, *Laws of Chaos* (Birkhäuser, Boston, 1997). While the theorems in this reference only apply to one dimensional maps, they extend to our model since the coordinate y plays a passive role in the forward dynamics.
 [20] S. Tasaki, T. Gilbert and J. R. Dorfman, *An Analytic Construction of the SRB Measures for Baker-type Maps*, Chaos **8**, 424 (1998).
 [21] Ya. Sinai, to appear in the proceedings of the NATO-ASI on Dynamics, Leiden, 1998, H.van Beijeren and J. Karkheck, eds.
 [22] S. Tasaki and P. Gaspard, in preparation.
 [23] T. Gilbert and J. R. Dorfman, *Hyperbolic and Non-hyperbolic Behavior in a Class of Non-linear Baker Maps*, in preparation.
 [24] T. Gilbert and J. R. Dorfman, in preparation.

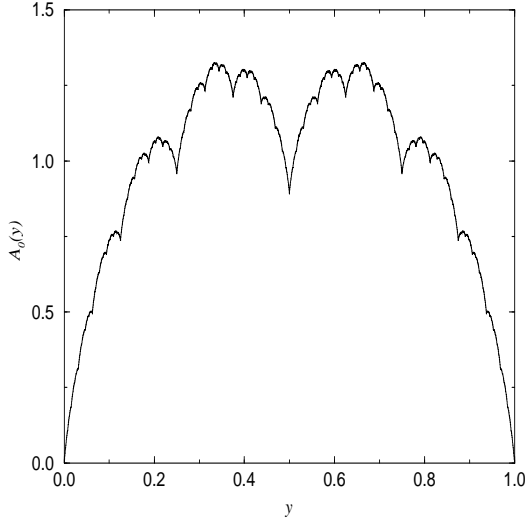


FIG. 1. $A_0(y)$ computed with a cut-off value $k_{max} = 250$.

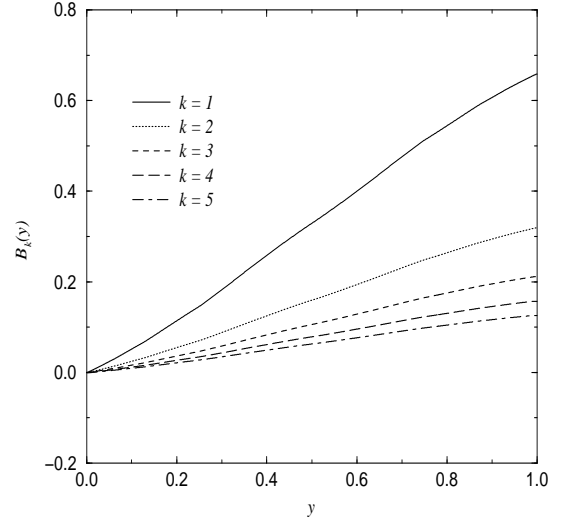


FIG. 3. The first five $B_k(y)$ computed with a cut-off value $k_{max} = 250$.

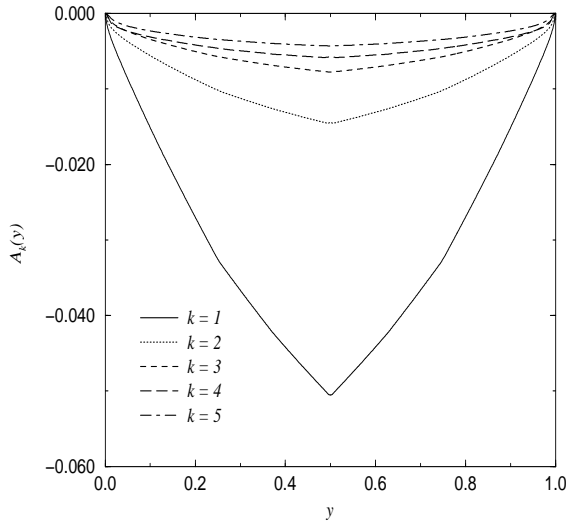


FIG. 2. The first five $A_k(y)$ computed with a cut-off value $k_{max} = 250$.

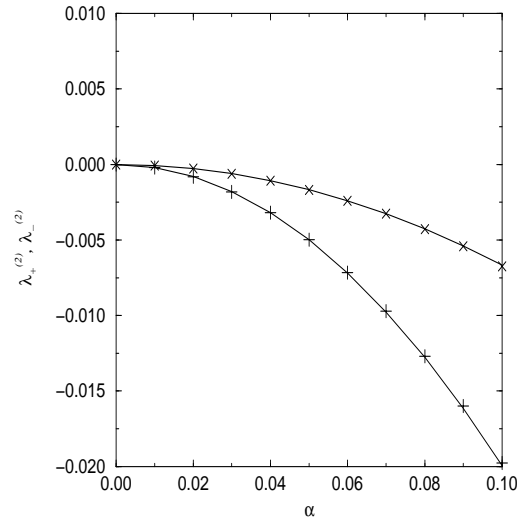


FIG. 4. A comparison of the values of the second order corrections of the Lyapunov exponents computed from Eqs. (19, 21) (solid lines) and by following a trajectory of 10000 steps for 10 values of α ranging from 0 to .1 (x's correspond to the positive Lyapunov exponent, +'s to the negative one).

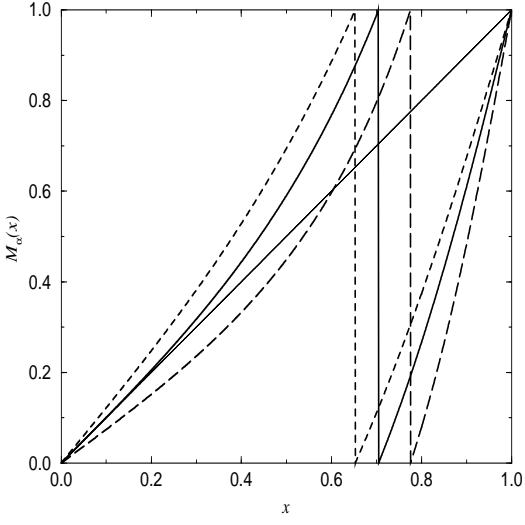


FIG. 5. M_α projected along the x -interval for $\alpha = .5$ (dashed line), $\ln(2)$ (solid line), 1 (long-dashed line). The origin goes from repelling to attractive as α increases above $\ln(2)$.